

# 688. Control of piezoelectric scanner dynamics using magnetorheological fluid

R. Bansevicius<sup>1</sup>, A. Bubulis<sup>2</sup>, E. Dragašius<sup>3</sup>, V. Jūrėnas<sup>4</sup>, V. Mačiukienė<sup>5</sup>, S. Navickaitė<sup>6</sup>

Kaunas University of Technology, Kaunas, Lithuania

E-mail: <sup>1</sup> ramutis.bansevicus@cr.ktu.lt, <sup>2</sup> alginantas.bubulis@ktu.lt,

<sup>3</sup> egidijus.dragasius@ktu.lt, <sup>4</sup> vytautas.jurenas@ktu.lt,

<sup>5</sup> viktorija.maciukiene@ktu.lt, <sup>6</sup> sigita.navickaite@stud.ktu.lt

(Received 21 September 2011; accepted 4 December 2011)

**Abstract.** The developed one-dimensional laser beam scanner, driven by a piezoelectric disc-type unimorph actuator is presented in this paper. The dynamics of a piezoelectric actuator is analyzed. A magnetorheological fluid (MRF) damper is used to eliminate transient vibrations of the scanner eigen frequencies induced by the stepped driving voltage. Experimental results demonstrate the effectiveness of the MRF damper in residual-vibration reduction in the laser beam scanner.

**Keywords:** piezoelectric actuator, scanner, dynamics, magnetorheological fluid (MRF).

## Introduction

Piezoelectric actuators can produce a relatively large force with very high efficiency and quick response speed [1]. In this paper, we present the design aspects of one-dimensional laser beam scanner. The scanner is composed of one single mirror, driven by unimorph piezoelectric actuator. A mirror tilted around two needle-like support springs, one of which is actuated by the disc-type unimorph, results in a compact fast steering laser scanner.

The operation speed and tracking accuracy of piezoelectric actuators in scanning process is significantly reduced due to the excitation of transient vibrations of the scanner eigen frequencies induced by the stepped driving voltages [2]. The time required for the transient vibrations to attenuate will depend upon the damping characters of the piezoelectric material and upon any external dampers that may be present in the structure. This paper presents a methodology of the residual vibration suppression for the repetitive fast-response and high-precision positioning in laser beam scanners using a magnetorheological fluid (MRF) damper.

Experimental results are presented that demonstrate the performance and effectiveness of the developed scanner.

This paper focuses on the design, fabrication and characterization of the disc-type unimorph actuators.

## Scheme and working principle of the piezoelectric scanner

Investigated piezoelectric scanner consists of disc-type unimorph actuator 2 and covered with disc shape metallic bearing 3, which are fixed by their perimeters in the frame 1. Its design is illustrated in Fig. 1. The optical beam mirror 4 is attached in the centre of the disc-type unimorph actuator 2 and bearing 3 using two needle-like supporting springs 5 and 6. The springs 5 and 6 have high rigidity in axial direction (perpendicular to a mirror surface) and low rigidity in lateral direction are fixed tightly to the piezoelectric actuator 2, bearing 3 and the optical beam mirror 4. Driven by unimorph piezoelectric actuator 2 through the needle-like

supporting spring 5, the mirror 4 is tilted around the stationary support 6. For the suppression of the residual vibrations of the piezoelectric actuator 2 the permanent magnet 7 with the drop 8 of a MRF is attached at the centre of the frame 1.

Bending deformations of the unimorph 2 can be actuated by the piezoelectric effect. Because of deformations of the unimorph 2, the optical beam mirror 4 can be turned in one direction by angle  $\alpha(t)$ .

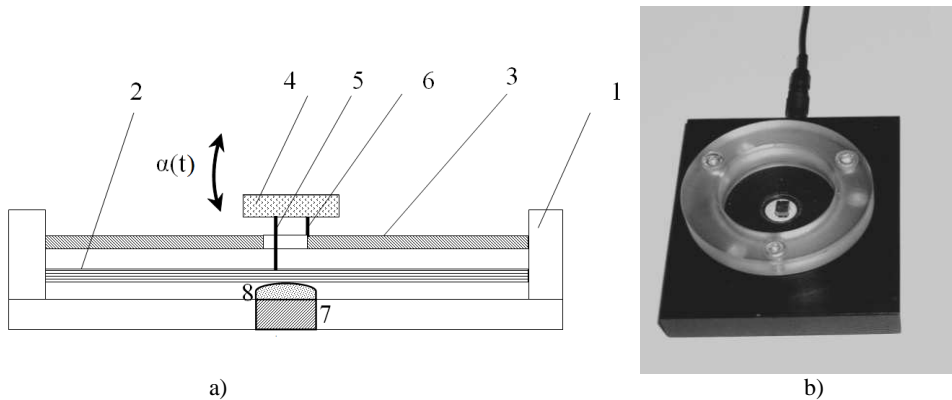


**Fig. 1.** The scheme (a) and photo (b) of the piezoelectric one-dimensional laser beam scanner: 1 – frame, 2 – disc-type unimorph, 3 – disc-type bearing, 4 – optical beam mirror, 5 and 6 – needle-like support springs of the mirror, 7 – permanent magnet, 8 – MRF

### Disc-type piezoelectric unimorph and MRF used in design of the piezoelectric scanner

A standard disc-type unimorph actuator is illustrated in Fig. 2. The actuator consists of a single piezoelectric layer, with radius  $r$ , bonded to a purely elastic layer, with radius  $R$ . Ferromagnetic steel is chosen for the elastic layer. When a voltage  $U$  is applied across the thickness of the piezoelectric layer, longitudinal and transverse strain develops. The elastic layer opposes the transverse strain which leads to a bending deformation.

The piezoelectric material used for the unimorph is PZT type Pz27 (Noliac A/S). As elastic layer is used ferromagnetic steel. The properties of materials are given in Table 1.

**Table 1.** Properties of PZT material Pz27 and steel.

Property	Values of PZT	Values of steel	Unit
Density	$7.7 \times 10^3$	$7.872 \times 10^3$	$\text{kg m}^{-3}$
Dielectric constant	1800		
Coupling factor	0.47		
$d_{31}$ charge constant	$-170 \times 10^{-12}$		$\text{m V}^{-1}$
Young's modulus	$45 \times 10^9$	$193 \times 10^9$	Pa
Mechanical quality factor	80		

The outer surfaces of the unimorph are plated with a layer of nickel electrodes, approximately  $2 \mu\text{m}$  thick. The unimorph (Fig. 1.) is driven into bending vibration by applying

an AC voltage  $U$  across the electrodes whose peak to peak amplitude is 6 V. Geometrical parameters of the scanner with the piezoelectric unimorph and permanent magnet (Neodymium magnet, flux density  $B=1,2$  T) are listed in table 2.

**Table 2.** Geometric parameters of the disc-type unimorph

R, mm	r, mm	$t_p$ , mm	$t_{np}$ , mm
8	5	0.1	0.21

In this paper authors investigate position control of piezoelectric unimorph for laser shutting system using MRF and magnetic forces.

**Table 3.** Properties of MRF used in experiments

MRF	MRF-122EG
Appearance	Dark grey liquid
Viscosity, Pa-s @ 40°C (104°F), Calculated as slope 800-1200 sec <sup>-1</sup>	0.042 ± 0.020
Density g/cm <sup>3</sup>	2.28-2.48
Solids Content by Weight, %	72
Flash Point, °C (°F)	>150 (>302)
Operating Temperature, °C (°F)	-40 to +130 (-40 to +266)

### Theoretical analysis

Seeking to find frequencies and maximum displacements of the disc-type unimorph used in investigated scanner we apply the following calculation methodology.

We consider a piezoelectric–nonpiezoelectric unimorph with a piezoelectric layer of thickness  $t_p$  and Young’s modulus  $E_p$  and a nonpiezoelectric layer of thickness  $t_{np}$  and Young’s modulus  $E_{np}$ , as schematically shown in Fig. 2. The bonding layer between the piezoelectric and nonpiezoelectric layers is neglected in this theory. A perfect bonding between the two layers is assumed. When an electric field  $E$  is applied in the  $z$  (thickness) direction, a lateral strain  $d_{31}E$  is generated in the piezoelectric layer, here  $d_{31}$  is the piezoelectric coefficient of the piezoelectric layer, causing the unimorph to bend. The position of a neutral plane,  $t_n$ , is determined by [5]:

$$\int_{-t_{np}}^0 E_{np} \left( \frac{z-t_n}{r} \right) dz + \int_0^{t_p} E_p \left( \frac{z-t_n}{r} \right) dz = 0 \quad (1)$$

where  $r$  is the radius of curvature due to bending. Once the position of the neutral plane is known, the bending modulus per unit length,  $D$ , of the piezoelectric–nonpiezoelectric unimorph can be calculated, according to [5]:

$$D = \int_{-t_{np}}^0 E_{np} (z-t_n)^2 dz + \int_0^{t_p} E_p (z-t_n)^2 dz \quad (2)$$

Bending modulus:

$$D = \frac{E_p^2 t_p^4 + E_{np}^2 t_{np}^4 + 2E_p E_{np} t_p t_{np} (2t_p^2 + 2t_{np}^2 + 3t_p t_{np})}{12(E_p t_p + E_{np} t_{np})} \quad (3)$$

The bending moments per unit length in the x and y directions  $M_{x,p}$  and  $M_{y,p}$ , resulting from the piezoelectric layer, and  $M_{x,np}$  and  $M_{y,np}$ , resulting from the nonpiezoelectric layer, can be calculated according to [5]:

$$M_{x,p} = M_{y,p} = \int_0^{t_p} E_p (d_{31}E - c)(z - t_n) dz = \frac{E_{np}t_{np}}{(E_{np}t_{np} + E_p t_p)} M_E$$

$$M_{x,np} = M_{y,np} = \int_{-t_{np}}^0 E_{np} (-c)(z - t_n) dz = \frac{E_p t_p}{(E_{np}t_{np} + E_p t_p)} M_E \quad (4)$$

where:

$$M_E = \frac{E_p E_{np} t_p t_{np} (t_p + t_{np}) d_{31} E}{2(E_{np}t_{np} + E_p t_p)} \quad (5)$$

And  $c$  is the in-plane constrain that satisfies [5]:

$$\int_{-t_{np}}^0 E_{np} c dz + \int_0^{t_p} E_p (c - d_{31}E) dz = 0 \quad (6)$$

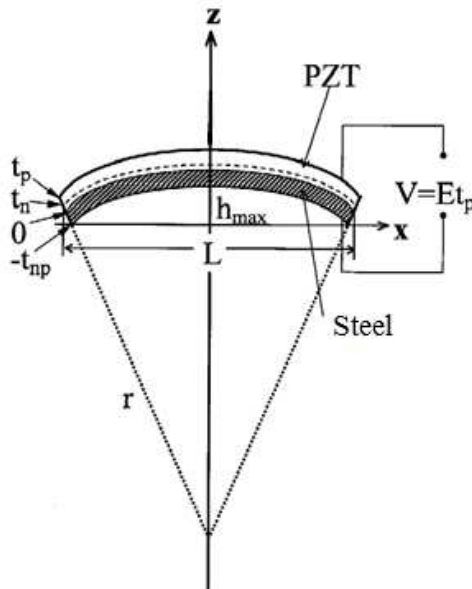


**Fig. 2.** Schematic view and coordinates of the disc-type unimorph [5]

For disc-type unimorphs, the displacement in  $z$  direction obeys the following differential equation [5]:

$$\left( \frac{\partial^2}{\partial r^2} + \frac{1}{r} \frac{\partial}{\partial r} + \frac{1}{r^2} \frac{\partial^2}{\partial \Theta^2} \right) h = -\frac{M'}{D} \quad (7)$$

where  $D$  is the bending modulus per unit length as defined in Eq. (3) and  $M'$  the bending modulus as defined in Eqs. (4) – (5),  $r$  – radius of piezoelectric element,  $R$  – radius of nonpiezoelectric material element. The solution of Eq. (7) is [5]:

$$h = \frac{M'}{4D}(R^2 - r^2) \quad (8)$$

when the disc-type unimorph is simply supported at the rim. The maximum displacement  $h_{\max}$  occurs at the center and is given by the following expression [2]:

$$h_{\max} = \frac{M'}{4D}R^2 = \frac{M'}{16D}L^2 = \frac{L^2}{8} \frac{6E_p E_{np} t_p t_{np} (t_p + t_{np}) d_{31} E (1 - \nu)}{E_p^2 t_p^4 + E_{np}^2 t_{np}^4 + 2E_p E_{np} t_p t_{np} (2t_p^2 + 2t_{np}^2 + 3t_p t_{np})} \quad (9)$$

The bending-mode vibration of the unimorph obeys the following differential equation [5]:

$$D' \nabla^2 \nabla^2 h = -m \frac{\partial^2 h}{\partial t^2} \quad (10)$$

where:

$$D' = \frac{1}{1 - \nu_{np}^2} \int_{-t_{np}}^0 E_{np} (z - t_n)^2 dz + \frac{1}{1 - \nu_p^2} \int_0^{t_p} E_p (z - t_n)^2 dz \quad (11)$$

and

$$m = \rho_p t_p + \rho_{np} t_{np} \quad (12)$$

In Eqs. (11) and (12),  $\rho_p$  and  $\rho_{np}$  are the densities of the piezoelectric and nonpiezoelectric layers, respectively and  $\nu_p$ ,  $\nu_{np}$ ,  $\nu$  are Poisson's ratios. In general, the resonance frequency of a plate obeys the following form [5]:

$$f = \frac{1}{2\pi} \left( \frac{\lambda}{L} \right)^2 \sqrt{\frac{D'}{m}} \quad (13)$$

where  $\lambda$  is the eigenvalue of Eq. (10), is dimensionless, and depends only on the shape of the plate and the boundary conditions. If we consider  $\nu_p = \nu_{np} = \nu$  and  $D' = D/(1 - \nu^2)$ , then we obtain [5]:

$$f = \frac{1}{2\pi} \left( \frac{\lambda}{L} \right)^2 \sqrt{\frac{E_p^2 t_p^4 + E_{np}^2 t_{np}^4 + 2E_p E_{np} t_p t_{np} (2t_p^2 + 2t_{np}^2 + 3t_p t_{np})}{12(E_p t_p + E_{np} t_{np})(\rho_p t_p + \rho_{np} t_{np})(1 - \nu^2)}}} \quad (14)$$

### Experimental study of piezoelectric scanner

In order to design laser scanner from a mechanical point of view, it is necessary to characterize its dynamic properties. The performance of the scanner has been evaluated through the experimental testing of various mirror displacement amplitudes and frequencies.

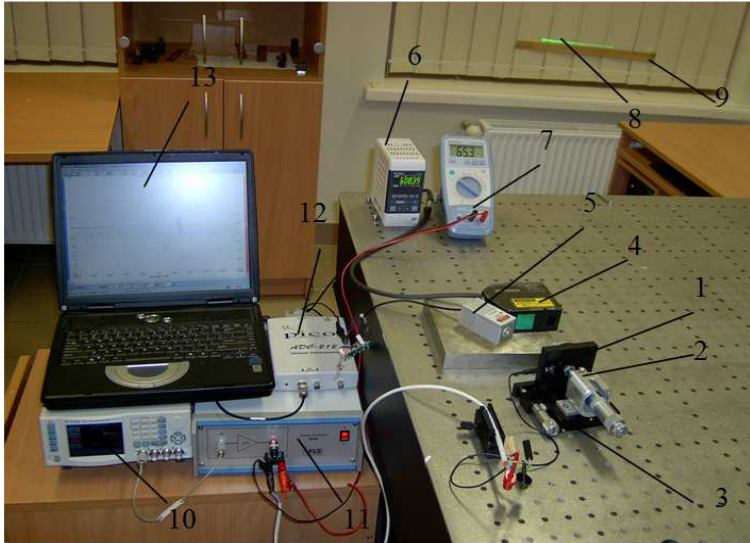


**Fig. 3.** Experimental set up: 1 – scanner; 2 – micrometric screw; 3 – holder of micrometric screw; 4 – laser displacement sensor LK-G82; 5 – He-Ne laser; 6 – laser sensor controller LK-G3001PV; 7 – multimeter Mastech 8201H; 8 – path of the scanned laser beam; 9 – ruler; 10 – signal generator Waveform generator WW5064; 11 – voltage amplifier P-200; 12 – analog digital converter ADC-212; 13 – computer

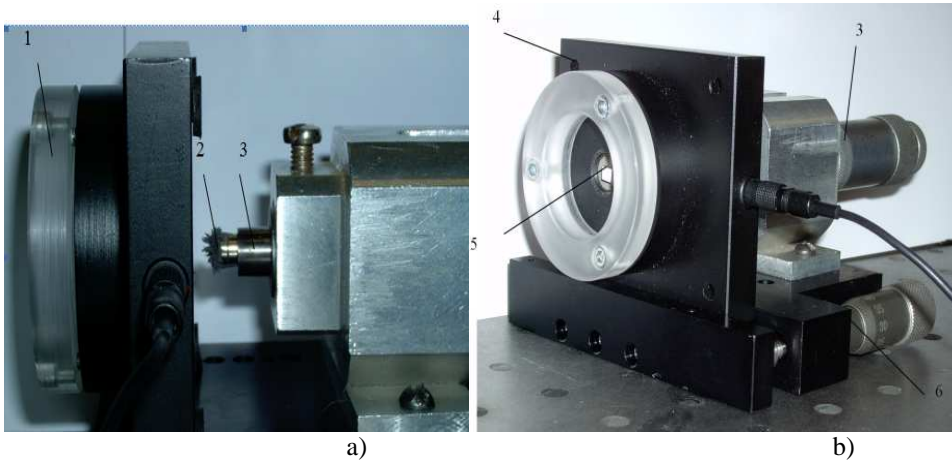


**Fig. 4.** The view of scanner: 1 – scanner, 2 – MRS with magnet, 3 – micrometer, 4 – frame of the scanner, 5 – mirror, 6 – holder of micrometric screw

An experimental investigation was carried out for optomechanical characterization of the device. He–Ne laser was reflected off a mirror positioned at 45° and then projected onto a position-sensitive detector. A function generator and amplifier were used to drive the devices using a maximum voltage of 20 V in total amplitude (Fig. 3). The driving voltage and detector output were recorded by a digital oscilloscope and saved to a computer for analysis. The quasi-static response and hysteresis of mirror motion angle were determined with vibrations frequency of 0.5 Hz to provide the largest displacement of the mirror.

The experimental results demonstrate the effectiveness of the MRF damper in residual-vibration reduction in the laser beam scanner (Fig. 5 and Fig. 7).

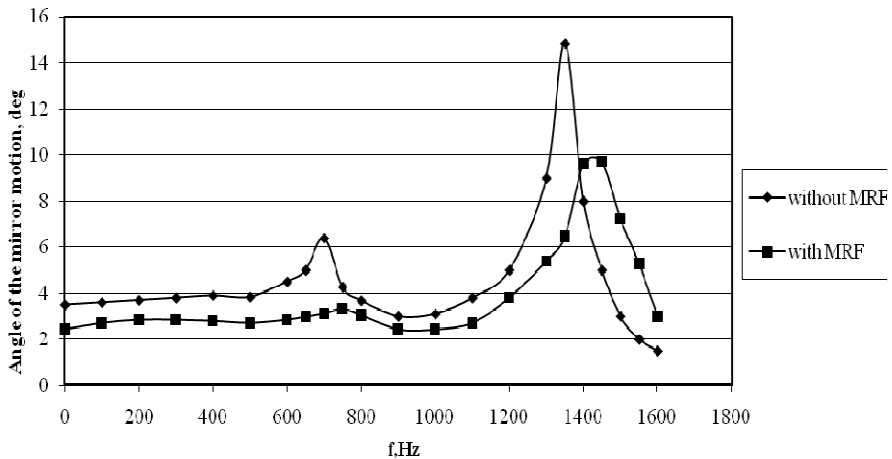


Fig. 5. Amplitude – frequency responses of the piezoelectric scanner with and without MRF

Because the piezoelectric mirrors were actuated by AC voltage, we verified that voltage of opposite sign corresponded to the angular displacement exhibits reproducible hysteresis as expected from a piezoelectrically actuated device. Electrical compensation could be used to minimize the impact of hysteresis of mirror tilt angle (Fig. 6).

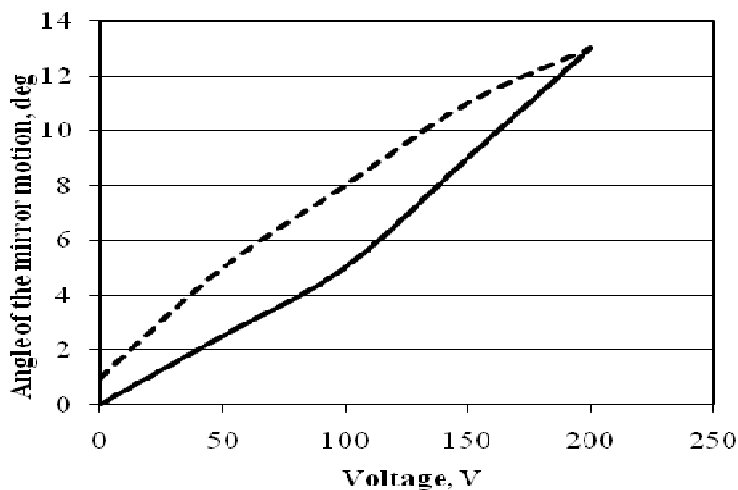
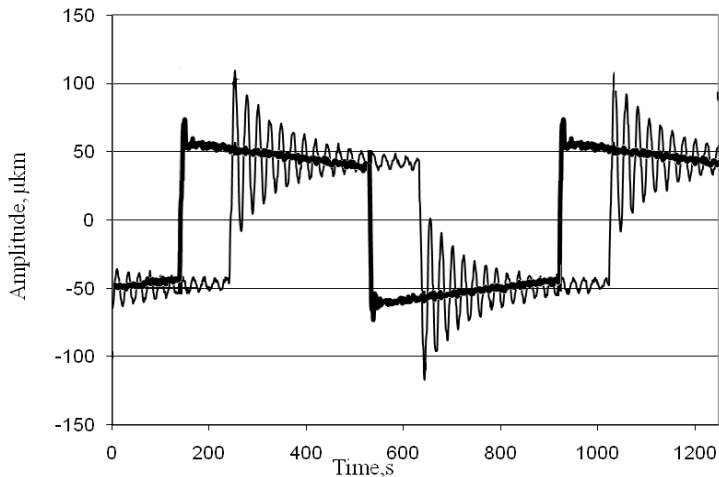


Fig. 6. Hysteresis of mirror motion angle with respect to operating voltage

Applying the MRF damper for the scanner provides improved performance and reduces the residual vibrations from a step motion of the mirror.



**Fig. 7.** Experimental results of step response of scanner with and without MRF damper

It has been demonstrated that the above MRF damper not only reduces the residual vibration, but also changes resonant frequency up to 10%.

## Conclusions

Experimental results demonstrate the effectiveness of the MRF damper in residual-vibration reduction in the laser beam scanner driven by the stepped driving voltage. We have developed a 1D laser beam scanner with maximum beam deflection of  $16^\circ$  and a resonant frequency of 1413 Hz.

These types of devices can be applied to an array of optical systems, such as imaging and optical monitoring/tracking that require fine position control and real-time adaptability. We believe the developed device can provide a compact, low-cost and low-power solution for adaptive optical steering systems.

## Acknowledgements

This research was funded by a grant (No. 31V115) from the Lithuanian Agency of Science, Innovation and Technology.

## References

- [1] **Dong S., Bouchilloux Du X., Uchino K.** Ring Type Uni/BiMorph Piezoelectric Actuators, International Center for Actuators and Transducers, Materials Research Institute, The Pennsylvania State University, University Park, PA 16802, USA.
- [2] **Wang Q., Du X., Xu B., Cross L.** "Electromechanical coupling and output efficiency of piezoelectric bending actuators", IEEE Trans. on Ultrasonics, Ferro. and Freq. Control, Vol.46, May 1999, p. 638-646.

- [3] **Donoso A., Sigmund O.** Optimization of piezoelectric bimorph actuators with active damping for static and dynamic loads, E. T. S. Ingenieros Industriales Universidad de Castilla - La Mancha 13071 Ciudad Real, March 2007.
- [4] Data sheet of magnetorheological fluid MRF-122EG, LORD, USA.
- [5] **Li X., Shih W. Y., Akasy I. A., Shih W.** Electromechanical Behavior of PZT–Brass Unimorphs, Department of Materials Engineering, Drexel University, Philadelphia, Pennsylvania 19104-2875; and Department of Chemical Engineering and Princeton Materials Institute, Princeton University, Princeton, New Jersey 08544-5263.